

# Integrated Microwave Photonic Phase Shifter with Ultrahigh Dynamic Range

Kaixuan Ye<sup>(1)</sup>, Gaojian Liu<sup>(2)</sup>, Okky Daulay<sup>(1)</sup>, Marcel Hoekman<sup>(3)</sup>, Edwin J. Klein<sup>(3)</sup>, Chris Roeloffzen<sup>(3)</sup>,  
and David Marpaung<sup>(1)</sup>

<sup>(1)</sup> Nonlinear Nanophotonics Group, University of Twente, Enschede 7500 AE, the Netherlands  
[k.ye@utwente.nl](mailto:k.ye@utwente.nl)

<sup>(2)</sup> China Academy of Space Technology, Xi'an, China

<sup>(3)</sup> LioniX International BV, Enschede 7500 AL, the Netherlands

**Abstract** We experimentally demonstrate, for the first time to the best of our knowledge, an integrated microwave photonic phase shifter with ultra-high dynamic range. We achieved  $2\pi$  tunable phase shift with amplitude variation of  $< 1$  dB and a spurious-free dynamic range of  $121.6 \text{ dB} \cdot \text{Hz}^{4/5}$ . ©2022 The Author(s)

## Introduction

Integrated microwave photonic (MWP) phase shifter holds great promise in communication, sensing, and defense systems for its advantages of large bandwidth, low loss, and electromagnetic interference immunity<sup>[1]</sup>. Previous works have already demonstrated key functionalities such as the ultra-wide bandwidth<sup>[2],[3]</sup>, fast response time<sup>[4]</sup>, and small power variations<sup>[5]</sup>. However, the spurious-free dynamic range (SFDR), which is an important figure of merit to evaluate the linearity of the MWP system, is barely discussed in the integrated MWP phase shifter design.

The SFDR is the dynamic range of the RF power that can be accommodated in the MWP system with sufficient signal-to-noise ratio (SNR) and negligible intermodulation distortion<sup>[1]</sup>. Most previous methods to enhance the SFDR rely on additional lasers or modulators or waveshapers for spectral shaping, which would increase the cost and complexity of the system<sup>[6],[7]</sup>. Recently, we reported an on-chip linearization method with an integrated spectral shaper<sup>[8],[9]</sup>. It can be applied to synthesize an integrated MWP notch filter while achieving a record-high SFDR simultaneously<sup>[10]</sup>.

In this work, we show that the integrated spectral shaper can be reconfigured to realize a wide-band tunable phase shifter with world-record high SFDR. We apply two cascaded all-pass ring resonators at the over-coupled (OC) state to cover a  $2\pi$  phase shift with an amplitude variation of  $< 1$  dB. Moreover, by independently controlling the phase and amplitude of the carrier and the sidebands, the third-order intermodulation distortion (IMD3) terms from

different beating products destructively interfere with each other. Consequently, the IMD3 is suppressed by more than 34 dB, and an SFDR as high as  $121.6 \text{ dB} \cdot \text{Hz}^{4/5}$  is achieved. Our results point to the great potential of an MWP system with advanced functionality and high linearity.

## Working Principles

The proposed phase shifter is based on separating and independently shaping the optical carrier and  $2^{\text{nd}}$ -order sideband. The schematic and the signal flow of the experiment are shown in Fig. 1. First, light is sent to a phase modulator (PM). Because of the nonlinearity of the PM, multi-order sidebands would be generated. We filter out the lower sidebands but leave the optical carrier and both the  $1^{\text{st}}$ - and  $2^{\text{nd}}$ -order upper sidebands for further processing. For the linearization purpose (as explained later), we also suppress the optical carrier with the bandpass filter. After that, the signal is amplified with an erbium-doped fiber amplifier (EDFA) and coupled into the integrated spectral shaper.

The integrated spectral shaper consists of a spectral de-interleaver, a tunable attenuator, a phase shifter, a combiner, and two cascaded all-pass ring resonators<sup>[9]</sup>. The spectral de-interleaver spatially separates the  $2^{\text{nd}}$ -order upper sideband from the optical carrier and the  $1^{\text{st}}$ -order upper sideband. Then, the phase shift is introduced to the optical carrier with two cascaded all-pass ring resonators to achieve the MWP phase shifter function. The  $2^{\text{nd}}$ -order upper sideband is processed using a phase shifter and a tunable attenuator for linearization simultaneously with the phase shifter function. After that, the signals are recombined and converted to the RF

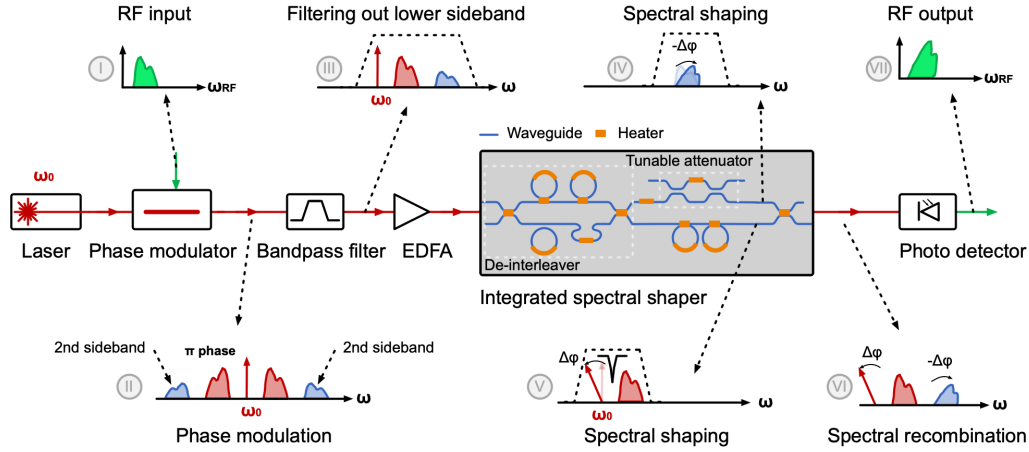


Fig. 1: Schematic and signal flow of the linearized integrated MWP phase shifter. EDFA: erbium-doped fiber amplifier.

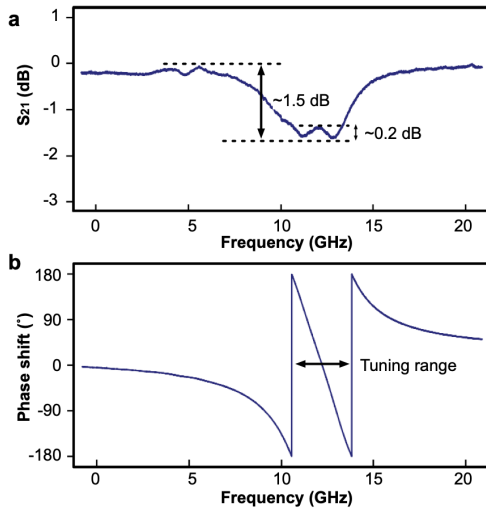


Fig. 2: a. Amplitude and b. phase response of the two cascaded all-pass ring resonators at the OC state.

domain with the photodetector.

The amplitude and phase responses of the cascaded all-pass ring resonators are shown in Fig. 2. Both rings are tuned to the OC state to create a total phase shift range of  $4\pi$ . To reduce the power variation at different phase shift, the notches are tuned to be close to each other and only the bottom of the stopband with variation  $< 0.2$  dB is used for phase shifting.

### Linearization Method

Because of the nonlinearity of the MWP systems, higher-order sidebands are always generated along with the first-order sidebands, which would be converted to the intermodulation distortion signals, e.g., IMD3, in the RF domain, and limit the SFDR of the system.

One effective way to enhance the SFDR is to independently shape the amplitude and the phase of the optical carrier and sidebands, and let the IMD3 from different beating products destructively interfere with each other. The RF

signal at the photo detector is:

$$I_{PD}(t) = R_{PD} |E_p(t)|^2 = I_1 \cos \omega_{\text{fund}1,2} t + I_3 \cos \omega_{\text{IMD}3,2} t \quad (1)$$

Where  $R_{PD}$  is the responsivity of the photo detector,  $E_p$  is the electric field of the light at the photodetector, and  $\omega_{\text{fund}1,2}$  and  $\omega_{\text{IMD}3,2}$  are the frequencies of the fundamental tones and IMD3 respectively. The electric field at the photo detector in the proposed phase shifter can be approximately expressed as<sup>[8]</sup>:

$$E_p = \sqrt{P_i} \cdot e^{j\omega_0 t} \left\{ \begin{array}{l} \alpha_0 J_0^2 e^{j\Delta\varphi_0} + \alpha_2 J_0 J_2 e^{j(2\omega_{\text{fund}1,2} t + \Delta\varphi_2)} \\ -\alpha_0 J_1^2 e^{j(\omega_{\text{IMD}2} t + \Delta\varphi_0)} + J_0 J_1 e^{j\omega_{\text{fund}1,2} t} \\ -J_1 J_2 e^{j\omega_{\text{IMD}3,2} t} \end{array} \right\} \quad (2)$$

Where  $P_i$  is the input optical power,  $\omega_0$  is the frequency of the carrier,  $\omega_{\text{IMD}2}$  is the frequency difference between the two fundamental tones,  $\alpha_0$  and  $\alpha_2$  are the amplitude attenuation of the carrier and the 2<sup>nd</sup>-order sideband,  $\Delta\varphi_0$  and  $\Delta\varphi_2$  are the phase shift of the carrier and the 2<sup>nd</sup>-order sideband, and  $J_n$  is the  $n$ -th order Bessel function of the first kind.

Applying (2) into (1) and taking the small-signal approximation, we find that the IMD3 terms can be perfectly canceled when the attenuation and phase shift imposed to the optical carrier and 2<sup>nd</sup>-order sideband satisfy the condition:

$$\left\{ \begin{array}{l} \alpha_2 - 3\alpha_0 = 0 \\ \Delta\varphi_0 = -\Delta\varphi_2 \end{array} \right. \quad (3)$$

It means that the power attenuation at the optical carrier should be 9.54 dB larger than that of the +2 optical sideband, and the phase shift to the optical carrier and the 2<sup>nd</sup>-order sideband

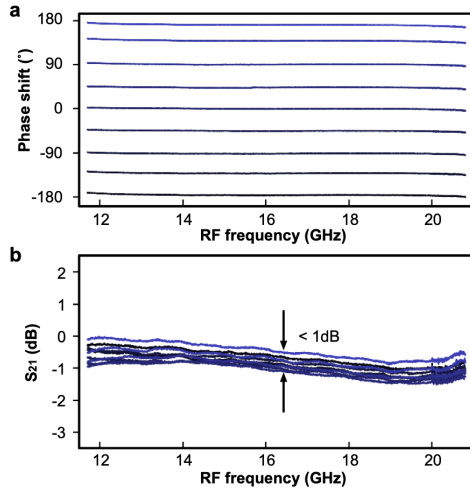


Fig. 3: a. Phase shift and b. power variation of the proposed phase shifter.

should be opposite to achieve the highest IMD3 rejection.

## Experiments

A series of experiments are performed to verify the feasibility of the proposed linearized phase shifter and the effectiveness of the linearization method. An optical carrier set at 1550 nm with an optical power of 18 dBm is emitted from a low relative-intensity noise (RIN) continuous wave (CW) laser (Pure Photonics PPCL550). The optical carrier is modulated using a PM (Thorlabs, 40 GHz) driven by an RF signal from a vector network analyzer (VNA, Keysight P5007A). The output of the PM is then sent to a bandpass filter (EXFO XTM-50) to filter out the lower sideband and introduce 9 dB attenuation to the optical carrier for the linearization method. Then, the phase modulation spectrum is amplified by a low-noise EDFA (Amonics) and injected into the  $\text{Si}_3\text{N}_4$  photonic chip (LioniX International BV). The free spectral range (FSR) of the on-chip de-interleaver and all-pass ring resonator is 160 GHz and 50 GHz, respectively.

By applying different voltages to corresponding heaters, the coupling coefficient and resonance frequency of the rings can be tuned to process the optical carrier and sidebands. The processed optical signal is sent to a photodetector (APIC 40 GHz) and the converted RF signal is measured with a VNA. For the SFDR measurement, the phase modulator is driven by a two-tone signal generated by RF signal generators (Wiltron 69147A and Rohde-Schwarz SMP02), and the converted RF signal is measured with an RF spectrum analyzer (Keysight N9000B).

Fig. 3 shows the phase and amplitude

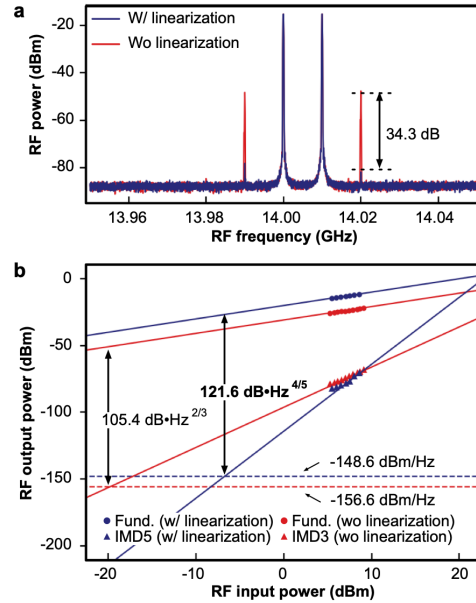


Fig. 4: a. Measured RF spectrum and b. SFDR of the phase shifter with and without linearization.

response of the proposed phase shifter. It can cover the  $2\pi$  phase shift range. The phase response is relatively flat from 12 to 20 GHz, and the amplitude variation at different phase shifts is  $< 1$  dB.

The measured RF spectrum and SFDR of the proposed phase shifter are shown in Fig. 4. As a comparison, we also show the spectrum and SFDR of a standard phase shifter without linearization, which is realized by changing the phase of the optical carrier with two cascaded all-pass ring resonators at the OC state. As shown in Fig. 4a, the IMD3 can be suppressed by  $> 34$  dB when the condition in (3) is satisfied after applying the linearization method to the system. Due to the cancellation of the IMD3, the IMD5 begins to dominate in the SFDR measurement, and a SFDR as high as  $121.6 \text{ dB} \cdot \text{Hz}^{4/5}$  is achieved.

## Conclusions

We have demonstrated, for the first time to the best of our knowledge, an integrated MWP phase shifter with the highest SFDR of  $121.6 \text{ dB} \cdot \text{Hz}^{4/5}$ . This result points to the great potential of an integrated MWP system with advanced functionality and high linearity.

## Acknowledgements

This work is supported by the Dutch NWO Vidi (15702) and Start-Up (740.018.021) grants.

## References

- [1] D. Marpaung, J. Yao, and J. Capmany, "Integrated microwave photonics", *Nature photonics*, vol. 13, no. 2, pp. 80–90, 2019. DOI: 10.1038/s41566-018-0310-5.

- [2] W. Liu and J. Yao, "Ultra-wideband microwave photonic phase shifter with a 360 tunable phase shift based on an erbium-ytterbium co-doped linearly chirped fbg", *Opt. Lett.*, vol. 39, no. 4, pp. 922–924, 2014. DOI: 10.1364/OL.39.000922.
- [3] L. McKay, M. Merklein, A. C. Bedoya, *et al.*, "Brillouin-based phase shifter in a silicon waveguide", *Optica*, vol. 6, no. 7, pp. 907–913, 2019. DOI: 10.1364/OPTICA.6.000907.
- [4] C. Porzi, G. Serafino, M. Sans, *et al.*, "Photonic integrated microwave phase shifter up to the mm-wave band with fast response time in silicon-on-insulator technology", *Journal of Lightwave Technology*, vol. 36, no. 19, pp. 4494–4500, 2018. DOI: 10.1109/JLT.2018.2846288.
- [5] Q. Shang, Y. Yu, Y. Zhang, *et al.*, "A silicon photonic rf phase shifter with linear phase response and low rf power variation", *IEEE Photonics Technology Letters*, vol. 31, no. 9, pp. 713–716, 2019. DOI: 10.1109/LPT.2019.2906373.
- [6] Y. Gu and J. Yao, "Microwave photonic link with improved dynamic range through pi phase shift of the optical carrier band", *Journal of Lightwave Technology*, vol. 37, no. 3, pp. 964–970, 2019. DOI: 10.1109/JLT.2018.2884350.
- [7] Y. Bai, X. Song, Z. Su, *et al.*, "Large dynamic range microwave photonic phase shifter based on multi-order sidebands optical spectrum vector process technique", in *2021 Optical Fiber Communications Conference and Exhibition (OFC)*, 2021, pp. 1–3.
- [8] G. Liu, O. Daulay, Y. Klaver, *et al.*, "Integrated microwave photonic spectral shaping for linearization and spurious-free dynamic range enhancement", *Journal of Lightwave Technology*, vol. 39, no. 24, pp. 7551–7562, 2021. DOI: 10.1109/JLT.2021.3093201.
- [9] X. Guo, Y. Liu, T. Yin, *et al.*, "Versatile silicon microwave photonic spectral shaper", *APL Photonics*, vol. 6, no. 3, p. 036106, 2021. DOI: 10.1063/5.0033516.
- [10] O. Daulay, G. Liu, K. Ye, *et al.*, "Ultrahigh dynamic range and low noise figure programmable integrated microwave photonic filter", *arXiv preprint arXiv:2203.04724*, 2022. DOI: 10.48550/arXiv.2203.04724.